Statistics of Tumbling of a Single Polymer Molecule in Shear Flow

Sergiy Gerashchenko and Victor Steinberg

Department of Physics of Complex Systems, Weizmann Institute of Science, Rehovot, 76100 Israel

(Received 9 March 2005; published 25 January 2006)

We present experimental results on statistics of polymer orientation angles relative to the shear plane and tumbling times in shear flow with thermal noise. The strong deviation of the probability distribution functions (PDFs) of the orientation angles from Gaussian PDFs was observed in good accord with theory. A universal exponential PDF tail for the tumbling times and its predicted scaling with Wi (that is, the dimensionless shear rate normalized by the polymer relaxation time) are also tested experimentally against numerics. The scaling relations of PDF widths for both angles as a function of Wi are verified and compared with numerics.

DOI: 10.1103/PhysRevLett.96.038304 PACS numbers: 83.80.Rs, 83.50.Ax

The dynamics and statistics of a single polymer molecule in stationary as well as in random flows have recently attracted the attention of both experimentalists [1–4] and theorists [5–10]. Stretching dynamics and statistics and coil-stretch transition in these flows were investigated in detail. Besides, another remarkable effect was first observed in a shear flow [2], namely, large fluctuations in a polymer elongation due to end-to-end aperiodic tumbling [see Fig. 1(d)]. The majority of orientation fluctuations occur in the vicinity of a direction determined by the shear, whereas sometimes they are interrupted by the flips in which the polymer orientation is reversed.

Recently rather extensive theoretical [11,12] and numerical [13,14] efforts were conducted with the goal of understanding the statistics of the angular orientation of a polymer molecule and of the tumbling time in a random velocity field with a mean shear. Shear flow with a thermal noise was considered as a particular case. A role of thermal noise in tumbling and orientation statistics of a rodlike object in a shear flow of a suspension was first considered more than 30 yrs ago in Ref. [15]. Similar effect should also occur for vesicles, wormlike micelles, etc., and it is crucial to correctly describe the rheology of these complex fluids. The role of the Brownian fluctuations in the polymer dynamics and statistics was studied in numerical simulations [7], where, however, only the power spectral density and the statistics of polymer extension in a shear flow were investigated. An average polymer extension and angular orientation were also theoretically considered in Ref. [8], where the results of calculations were compared with light scattering measurements [16,17].

In this Letter we concentrate on the statistics of angular orientation and the tumbling time and scaling relations of their characteristics for a single DNA molecule in a shear flow, when thermal fluctuations are the main cause for tumbling.

It is well known that a probability distribution function (PDF) of the end-to-end vector $\vec{R}$ for a polymer described by a dumbbell model with a linear relaxation in a simple shear is Gaussian [7]. Nevertheless, PDFs of the polymer extension, $|\vec{R}| \equiv R$, as well as polymer angular orientation, are strongly non-Gaussian due to anisotropy introduced by the shear. A functional form of the PDF of the polymer extension in a shear flow was first identified experimentally [2] and then explained theoretically and numerically [7].

The major finding of the recent theory [11,12] is the prediction of an *intermittency phenomenon* in the statistics of a single polymer tumbling in a shear flow that results in either algebraic or exponential tails of the distribution of polymer angular orientations and tumbling times, respectively. Moreover, it was also shown that the intermediate asymptote of the angular polymer statistics bears some universal features independent of the nature of polymer random excitation [11,13,14]. This observation has a fundamental interest, since it is the simplest stochastic system

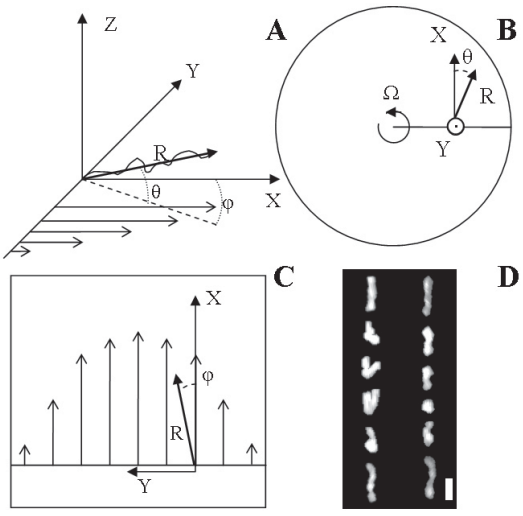

FIG. 1. (a) Polymer orientation angles in a shear flow; (b) Schematic diagram of rotating rod setup; (c) Schematic diagram of micro-channel setup; (d) Images of various polymer conformations consequent in time during tumbling. The white bar is 3.5 μm.

where nontrivial statistics appear as a result of white (Gaussian) noise. Recently considered systems, such as a passive scalar transport in a random Gaussian velocity field that also exhibit the intermittency, are described by a partial differential equation contrary to the current case, where the dynamics is governed by an ordinary differential (Langevin) equation [11].

The universal features of the orientation statistics are related to a deterministic nature of the angle evolution at large angles, where a random pumping can be neglected. Then the theory [11,12] predicts the following results on the angular distributions and tumbling time statistics: (i) at $|\phi| \gg \Delta\phi \sim \mathrm{Wi}^{-1}$ one gets $P(\phi) \propto (\sin\phi)^{-2}$, where $\Delta\phi$ is the width of $P(\phi)$, $\mathrm{Wi} = \dot{\gamma}\tau_{\mathrm{rel}}$ is the Weissenberg number, $\dot{\gamma}$ is the shear rate, and τ_{rel} is the polymer relaxation time; (ii) at $1 \gg |\theta| \gg \Delta\phi$ the PDF tail for θ is determined as $P(\theta) \propto |\theta|^{-2}$—both scalings follow from the deterministic process; (iii) the tail of PDF of tumbling time between two consequent flips, τ_ϕ, is exponential at $\tau_\phi \gg \tau_t$, where τ_t is the characteristic tumbling time that is proportional to τ_{rel}.

Another theoretical result verified by extensive numerical simulations based on linear dumbbell as well as finite extensible nonlinear elastic (FENE) models describes the scaling relations for the width of the angular distributions and the characteristic tumbling time with Wi [11–14]. The scaling is derived by simple physical arguments used by the theory [11,14]. The dynamic equation for one of the molecule orientation angles [see Fig. 1(a)], namely ϕ, in the region of $\phi \ll 1$ can be written as $\frac{d\phi}{dt} = -\dot{\gamma}\sin^2\phi + \frac{R_g}{R}(\tau_{\mathrm{rel}})^{-1/2}\eta_\phi$ [11–14], where R_g is the polymer gyration radius, and η_ϕ is the white thermal noise. In a stationary state one gets from a balance of shear and noise terms the following estimates for the rms of the angular fluctuations (or the PDF width), $\Delta\phi$, and the characteristic tumbling time, τ_t:

$$\Delta\phi \propto \mathrm{Wi}^{-1/3}\left(\frac{R_g}{R}\right)^{2/3}, \qquad \tau_t \propto \tau_{\mathrm{rel}}\mathrm{Wi}^{-2/3}\left(\frac{R_g}{R}\right)^{-2/3}. \tag{1}$$

Then one can consider two limits at $\mathrm{Wi} \gg 1$ (or small $\Delta\phi$ and $\Delta\theta$). In the linear extension limit, $R \ll R_{\max}$, where $R_{\max}$ is the maximum polymer extension, a typical polymer elongation, R, can be estimated as $R_g \times \mathrm{Wi}$ that is realized at sufficiently small extensions (up to 20% of $R_{\max}$ [1,4]). It leads to [11–14]

$$\Delta\phi \propto \mathrm{Wi}^{-1}, \qquad \tau_t \propto \tau_{\mathrm{rel}}. \tag{2}$$

In the opposite limit of a nonlinear regime, where typically $\mathrm{Wi} \geq R_{\max}/R_g$, a stretched polymer can be treated as a rigid rod with $R \sim R_{\max}$ subjected to the Brownian motion [15]. Then the resulting scaling appears to be strikingly different [11–14]:

$$\Delta\phi \propto \mathrm{Wi}^{-1/3}, \qquad \tau_t \propto \tau_{\mathrm{rel}}\mathrm{Wi}^{-2/3}. \tag{3}$$

Similar scalings can be also expected for $\Delta\theta$.

The experiments were carried out in a shear flow in two flow configurations. To measure θ we used a shear flow in a gap between the flat bottom of the uniformly rotating glass rod of radius $r_1 = 1.5$ mm and a cover slip (see, for details of the set-up, Ref. [4]). The measurements were made at the fixed height of ~ 30 μm above the cover glass in the region located at radius $r \simeq 700$ μm, where the main shear occurs in the vertical plane. Then only θ can be measured in this configuration [see Fig. 1(b)].

To measure ϕ a shear boundary layer of a Poiseuille flow in a micro-channel was used. The micro-channel of ~ 500 μm wide and ~ 100 μm deep was produced in elastomer (PDMS) by a soft lithography [18]. The measurements were carried out at about the middle height of the channel in a small region at a distance of ~ 30 μm from the channel wall, where only ϕ was detected via the cover glass [see Fig. 1(c)].

Particle image velocimetry (PIV) measurements were conducted with 0.2 μm fluorescent beads in both flow configurations. In the swirling flow the shear rate in the vertical plane is rather constant at the location of measurements of ~ 30 μm [Fig. 2(a)], while the azimuthal velocity in the horizontal plane almost independent of radius in the region of measurements [inset in Fig. 2(a)]. In the channel flow the longitudinal velocity measured in the horizontal plane changes rather linearly in the observation region of ~ 30 μm from the wall, while it looks fairly constant in the vertical plane at the middle height of the channel within the focus depth (0.4 μm) [see Fig. 2(b)]. In both cases the measured velocity profiles are compared with numerical calculations, and good quantitative agreement is found [solid lines, Figs. 2(a) and 2(b)]. A limitation to conduct PIV measurements in a vertical plane deeper than ~ 50 μm

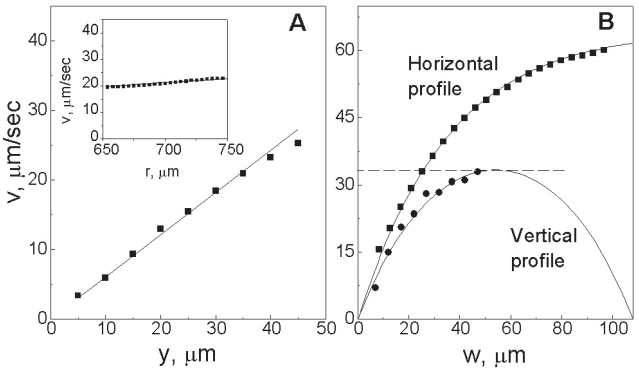

FIG. 2. (a) Azimuthal velocity vs vertical coordinate; inset: the same vs radius. Region of measurements is around $R = 700$ μm and at height of ~ 30 μm. (b) Squares are longitudinal velocity in the horizontal plane, and circles are the same in the vertical plane. Region of measurements at 30 ± 10 μm from the channel wall and at height of ~ 50 μm (dashed line). Solid lines on all plots are theoretical.

in both geometries is due to the objective working distance that is about 200 μm.

As a working fluid a buffer solvent [19] with sucrose concentration varied in the range between 47% (w/w) and 67% (w/w) to tune viscosity in the range between $\eta_s = 0.012$ Pa s and $\eta_s = 0.24$ Pa s at the working temperature of 22.5 °C was used.

To study the tumbling dynamics and statistics of polymer molecules in a flow 10^{-3} ppm of λ-DNA molecules, fluorescently labeled with YOYO-1 (Molecular Probes) at a dye/base ratio of 1:4 for ~1 h, were added into the solvent. At equilibrium the coiled λ DNA has $R_g = 0.73$ μm, while the entire contour length is $R_{\max} \approx 21$ μm. So it may be considered as a "flexible" polymer with roughly 300 persistence lengths [1]. The maximum relaxation time relevant for further analysis, $\tau_{\text{rel}} = 11 \pm 0.1$ sec for a solvent with 62% (w/w) sucrose was found. τ_{rel} for solvents with different sucrose concentrations was taken proportional to its concentration variation [1,2]. Fluorescently labeled DNA molecules were monitored via ×63, 1.4 numerical aperture oil immersion objective (Zeiss) with 0.4 μm depth of focus with a homemade inverted epifluorescent microscope [4]. Images of the molecules were digitized, and their θ and ϕ angles were automatically measured by approximation of a molecule outline with an ellipse, which main axis was used as the end-to-end vector, $\vec{R}$, to define an inclination angle, either θ or ϕ depending on the flow configuration [see Figs. 1(a)–1(c)]. This approximation works well for sufficiently stretched molecules down to 2–3 μm for the main axis. Two time series of different scenarios of tumbling that occur in a shear flow are presented in Fig. 1(d). One mentions that tumbling can take a place via coiled as well as folded states.

In the lower inset in Fig. 3 we present PDFs of θ for two values of Wi. Each plot is based on up to 30 000 points. It is clearly seen that at low Wi = 1.6 PDF can be fitted as Gaussian PDF almost entirely, while at high Wi = 17.6 the PDF tails strongly deviate from Gaussian. In Fig. 3 PDFs for three values of Wi are presented in the logarithmic coordinates. The PDF tails for all values of Wi decay algebraically with the exponent rather close to the theoretical, $|\theta|^{-2}$, indicated by a solid line on the plot. The larger the Wi, the wider the scaling region at the tail as predicted by the theory [11]. Variations in Wi values were achieved by viscosity tuning as well as variation in $\dot{\gamma}$ by changing rotation speed Ω between 0 and 0.7 sec^{-1}. The half-height width of PDFs, $\Delta\theta$, decreases as $\propto \text{Wi}^{-0.38\pm0.03}$ (see the upper inset in Fig. 3) in a rather good agreement with the recent numerical simulations based on the FENE model [14].

In the same setup with the rotating rod we measured PDFs of the tumbling time $P(\tau)$, determined in the experiment as time between two following consequent conformations: two coiled, two folded, or one coiled and one folded [see Fig. 1(d)]. This tumbling time, τ, is elongation

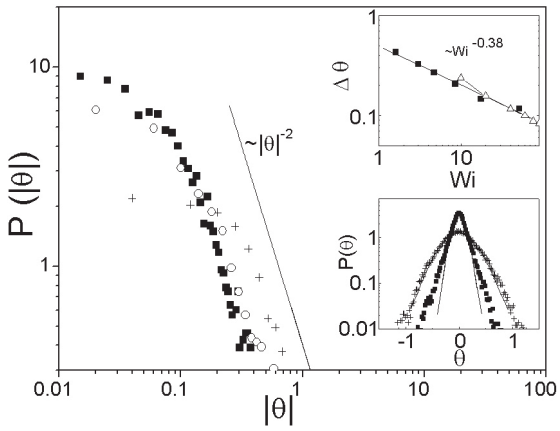

FIG. 3. PDFs of $|\theta|$ in logarithmic coordinates: Wi = 1.6 (pluses), Wi = 8.5 (circles), Wi = 17.6 (squares). A solid line is theoretically predicted asymptotic scaling for PDF tails. Lower inset: PDFs of θ for Wi = 1.6 (pluses), and Wi = 17.6 (squares) presented in log-linear coordinates; the solid curves are Gaussian fits. Upper inset: $\Delta\theta$ vs Wi; squares: data, triangles: numerics. A solid line is the fit.

based time defined by a certain length threshold $R_{\text{th}} > R_g$, and it is different from τ_ϕ, which is angular based. The lower the threshold, the higher τ_t [14]. We present in Fig. 4 $P(\tau)$ for three values of Wi together with the exponential fits. Each plot is based on up to 600 points. The same data presented in the log-linear coordinates together with the fits demonstrate the fit quality (inset in Fig. 4).

Figure 5 shows the characteristic tumbling time, τ_t, obtained from the slopes of the PDF tails, versus Wi. The value τ_t depends on the threshold value R_{th}/R_g. Wi was varied in two ways: full squares present the data, where Wi

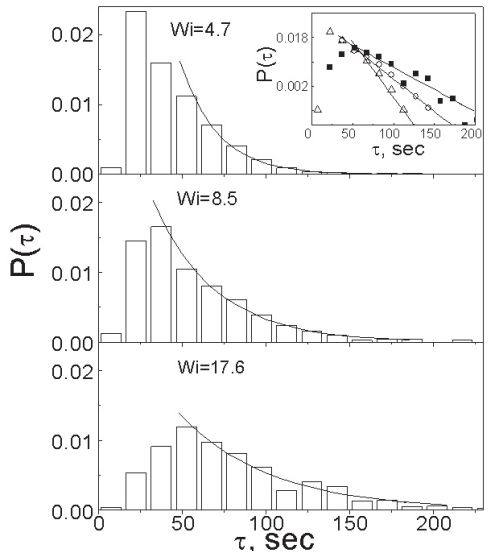

FIG. 4. PDFs of τ at several values of Wi. The solid lines are exponential fits. Inset: PDFs of τ in log-linear coordinates with fits to the data at Wi = 4.7 (triangles), Wi = 8.5 (circles), Wi = 17.6 (squares).

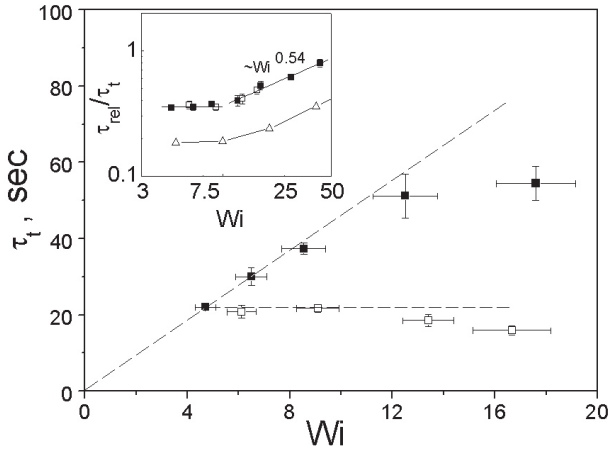

FIG. 5. τ_t vs Wi; full squares show data taken at constant s and varying viscosity; open squares represent data taken at constant viscosity and varying $\dot{\gamma}$. The dashed lines are guides to eye. Inset: $\tau_{\rm rel}/\tau_t$ vs Wi; triangles are numerics. Solid lines are the fits.

was tuned just by viscosity variation (it means the variation of $\tau_{\rm rel}$), and open squares were obtained at different Wi by adjusting $\dot{\gamma}$. By presenting the same data as the ratio $\tau_{\rm rel}/\tau_t$ versus Wi in the inset in Fig. 5 we show, first, that τ_t is proportional to $\tau_{\rm rel}$ at lower Wi, and second, $\tau_{\rm rel}/\tau_t$ grows as $\propto {\rm Wi}^{0.54\pm0.04}$ at higher Wi in a rather close agreement with numerical simulations [14]. The crossover region for scaling in τ_t takes place at ${\rm Wi} \simeq 10$ in amazing agreement between the experiment and the recent numerical simulations [14]. An apparent shift upwards of the data relative to the simulations (inset in Fig. 5) is explained by a value of $R_{\rm th}/R_g$ that is about twice smaller for the determination of τ in the simulations [14].

In Fig. 6 the PDF of ϕ measured in a micro-channel flow at ${\rm Wi} = 25$ together with the fit by $(\sin\phi)^{-2}$ are shown. It

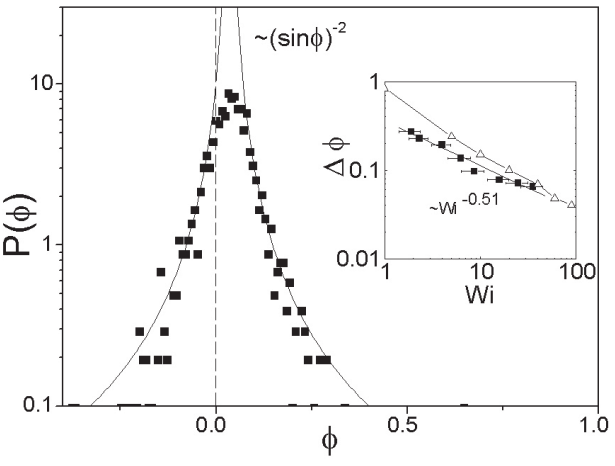

FIG. 6. PDFs of ϕ in log-linear coordinates at ${\rm Wi} = 25$. A solid curve is the fit by $\propto (\sin\phi)^{-2}$. Inset: $\Delta\phi$ vs Wi; squares are data, and triangles are numerics. A solid line is the fit.

is clear that the PDF maximum is located at $\phi_t \neq 0$ but limited angular resolution does not allow us to study its dependence on Wi. Similar data on $P(\phi)$, based on 2000–3000 points for each plot, were obtained for several values of Wi. The half-height width of PDFs, $\Delta\phi$, as a function of Wi is shown in the inset in Fig. 6 together with the fit and the results of the numerical simulations based on the FENE model [14]. The observed scaling $\propto {\rm Wi}^{-0.51\pm0.04}$ manifests the crossover region between $\propto {\rm Wi}^{-1/3}$ expected at high Wi and ${\rm Wi}^{-1}$ at lower Wi values [see Eqs. (2) and (3)].

We thank M. Chertkov, V. Lebedev, K. Turitsyn, A. Puliafito, and A. Celani for numerous discussions, exchange of results of the numerical calculations, and theoretical guidance, and E. Segre for help with software. This work was supported by the grants of Minerva Foundation, Israel Science Foundation, and by the Minerva Center for Nonlinear Physics of Complex Systems.

[1] T. Perkins, D. Smith, and S. Chu, Science **276**, 2016 (1997).
[2] D. Smith, H. Babcock, and S. Chu, Science **283**, 1724 (1999).
[3] J. Hur, E. Shaqfeh, H. Babcock, and S. Chu, Phys. Rev. E **66**, 011915 (2002); H. Babcock, R. Teixera, J. Hur, E. Shaqfeh, and S. Chu, Macromolecules **36**, 4544 (2003).
[4] S. Gerashchenko, C. Chevallard, and V. Steinberg, Europhys. Lett. **71**, 221 (2005).
[5] E. Balkovsky, A. Fouxon, and V. Lebedev, Phys. Rev. Lett. **84**, 4765 (2000).
[6] M. Chertkov, Phys. Rev. Lett. **84**, 4761 (2000).
[7] J. S. Hur, E. S. G. Shaqfeh, and R. G. Larson, J. Rheol. (N.Y.) **44**, 713 (2000).
[8] X. Wang and A. P. Chatterjee, Macromolecules **34**, 1118 (2001).
[9] B. Eckhardt, J. Kronjager, and J. Schumacher, Comput. Phys. Commun. **147**, 538 (2002).
[10] G. Boffetta, A. Celani, and S. Musacchio, Phys. Rev. Lett. **91**, 034501 (2003).
[11] M. Chertkov, I. Kolokolov, V. Lebedev, and K. Turitsyn, J. Fluid Mech. **531**, 251 (2005).
[12] K. Turitsyn (to be published).
[13] A. Puliafito and K. Turitsyn Physica (Amsterdam) **211D**, 9 (2005).
[14] A. Celani, A. Puliafito, and K. Turitsyn, Europhys. Lett. **70**, 464 (2005).
[15] E. J. Hinch and L. G. Leal, J. Fluid Mech. **52**, 683 (1972).
[16] A. Link and J. Springer, Macromolecules **26**, 464 (1993).
[17] E. C. Lee, M. J. Solomon, and S. J. Muller, Macromolecules **30**, 7313 (1997); E. C. Lee and S. J. Muller, Polymer **40**, 2501 (1999).
[18] Y. Xia and G. M. Whitesides, Angew. Chem., Int. Ed. **37**, 550 (1998).
[19] A pH8 buffer consisting of 10 mM tris-HCl, 2 mM EDTA, 10 mM NaCl, 4% β-mercaptoethanol, glucose oxidase ($\sim$50 μg/ml) and catalase ($\sim$10 μg/ml), 62% (w/w) sucrose was used (see, e.g., Ref. [1]).